

*Supporting information*

**Superior carbon belts from spirogyra for efficient extracellular  
electron transfer and sustainable microbial energy harvesting**

Yu-Tong Shi<sup>1,#</sup>, Yang-Yang Yu<sup>1,#</sup>, Zi-Ai Xu<sup>1</sup>, Jiabiao Lian<sup>2</sup>, Yang-Chun Yong<sup>1,3,\*</sup>

*<sup>1</sup>Biofuels Institute, School of Environment and Safety Engineering, Jiangsu University,  
301 Xuefu Road, Zhenjiang 212013, China*

*<sup>2</sup>Institute for Energy Research, Jiangsu University, Zhenjiang 212013, 301 Xuefu  
Road, Zhenjiang 212013, China*

*<sup>3</sup>Zhenjiang key laboratory of advanced sensing materials and devices, School of  
Mechanical Engineering, Jiangsu University, 301 Xuefu Road, Zhenjiang 212013,  
China*

#Equal contribution

\* Corresponding author, Email: [ycyong@ujs.edu.cn](mailto:ycyong@ujs.edu.cn); Fax: +86-511-8879 0955



**Figure S1.** (a) Fresh spirogyra aggregation collected from freshwater lake. (b) Dried spirogyra aggregation. (c) Picture of the single spirogyra filament.

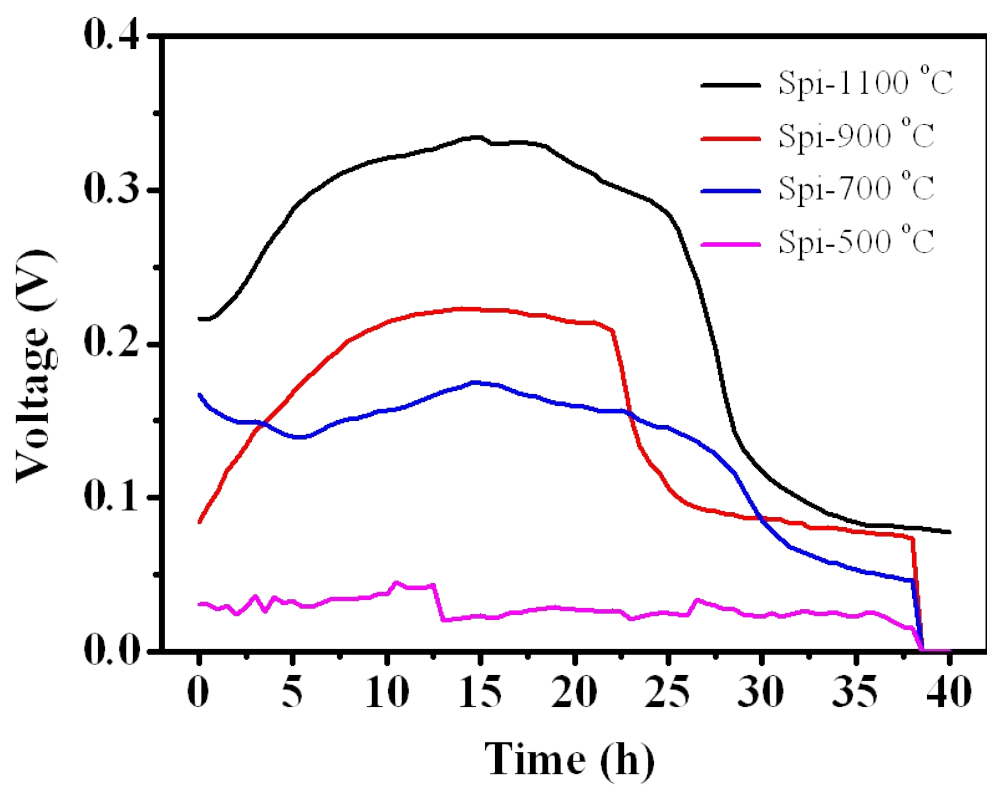


**Figure S2.** Voltage output of MFCs with spirogyra electrodes carbonized at different temperatures. According to the preliminary results, 1100 °C was further used for spirogyra carbonization.

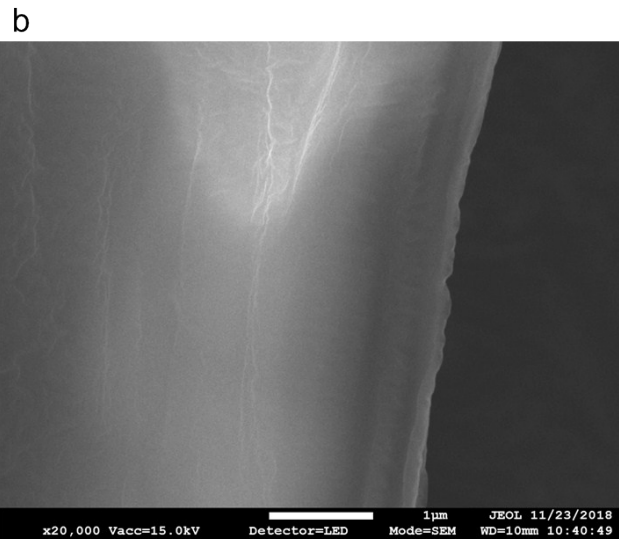
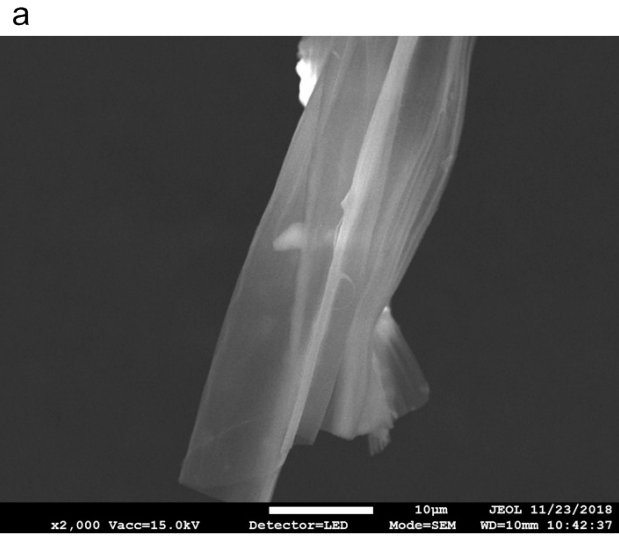


**Figure S3.** SEM images of the spirogyra filament after freezing drying at low (a) and high magnification (b). The images showed that filament surface was lightly wrinkled without nanoparticles coating.

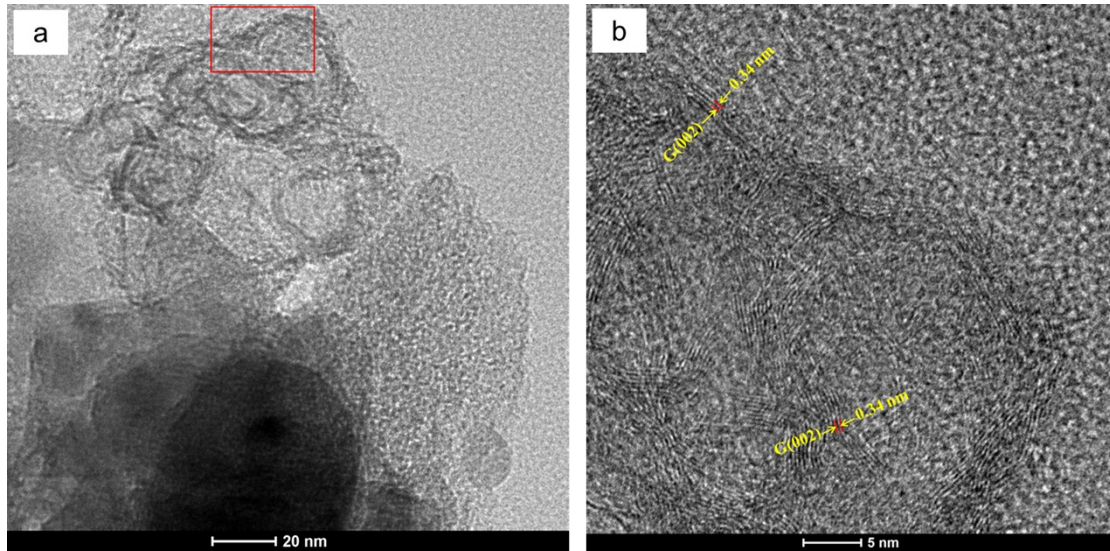


**Figure S4.** HR-TEM images of edge of the carbonized spirogyra micro-belt at low (a) and high (b) magnification. The red frame indicates the area magnified in (b). According to the high magnification HRTEM, the lattices corresponding to the crystal face (002) of graphite was observed. Moreover, few layers (3-10 layers) graphene-like structures could be observed under the high magnification (b).

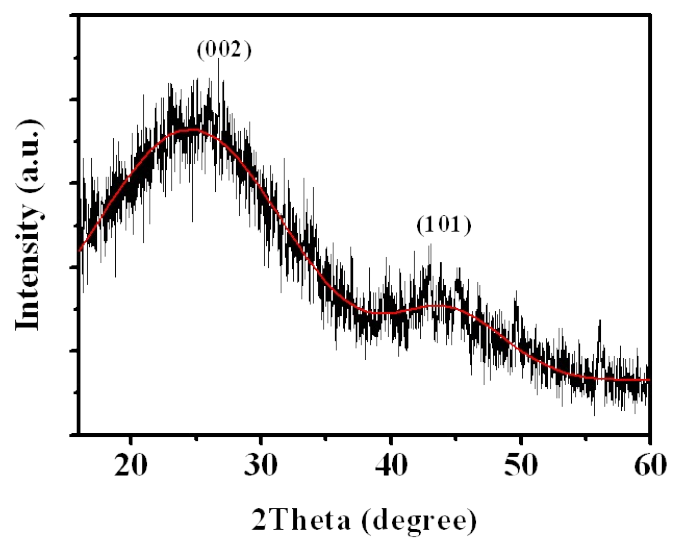


**Figure S5.** Powder XRD diffraction pattern of the carbonized spirogyra micro-belts.

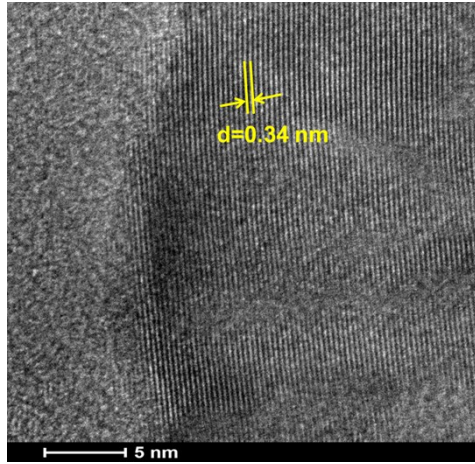


**Figure S6.** HR-TEM image of the carbonized spirogyra carbon belt.

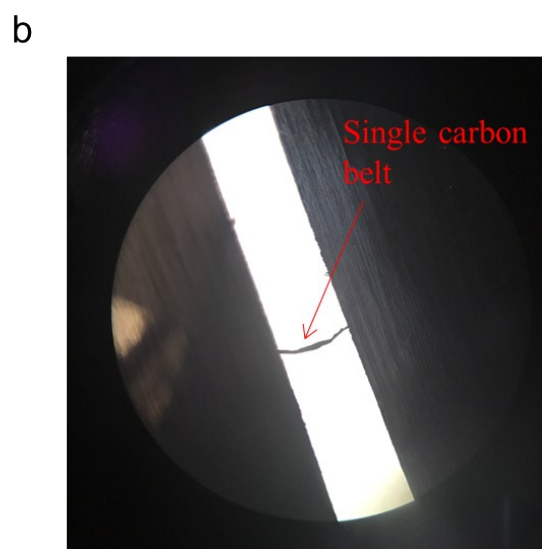
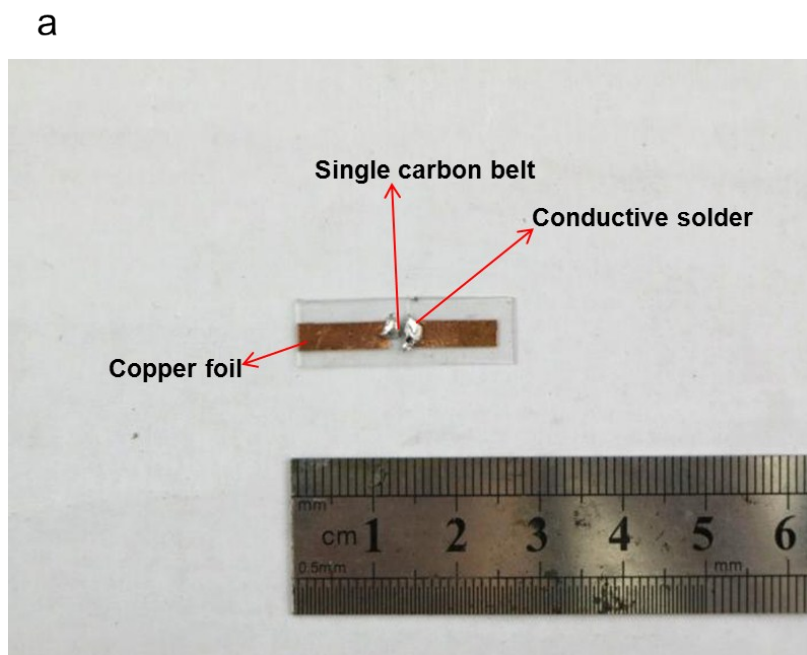


**Figure S7.** (a) The device used for measurement on the conductivity of single spirogyra carbon belt. (b) Magnified image of the device for clearly identification the single carbon belt in the device of (a).

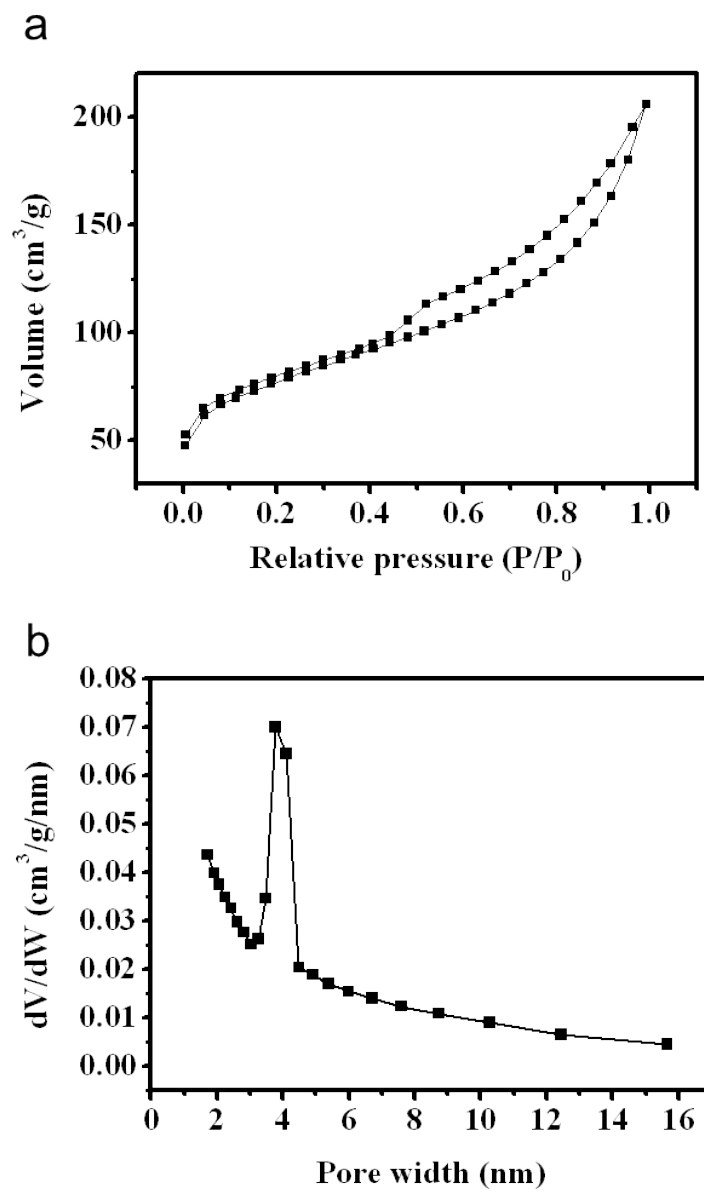


**Figure S8.** (a) Nitrogen adsorption-desorption isotherms for carbonized spirogyra micro-belt. (b) Pore size distribution for carbonized spirogyra carbon belt.

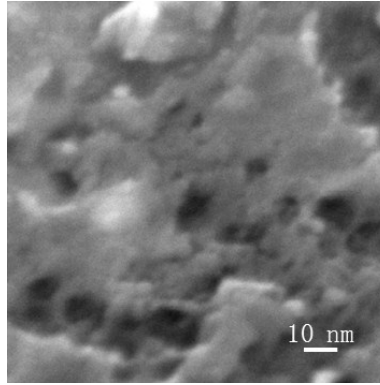


**Figure S9.** SEM image of the surface of the carbonized spirogyra micro-belt at high magnification. Mesopores on the surface of the carbon belt could be observed.

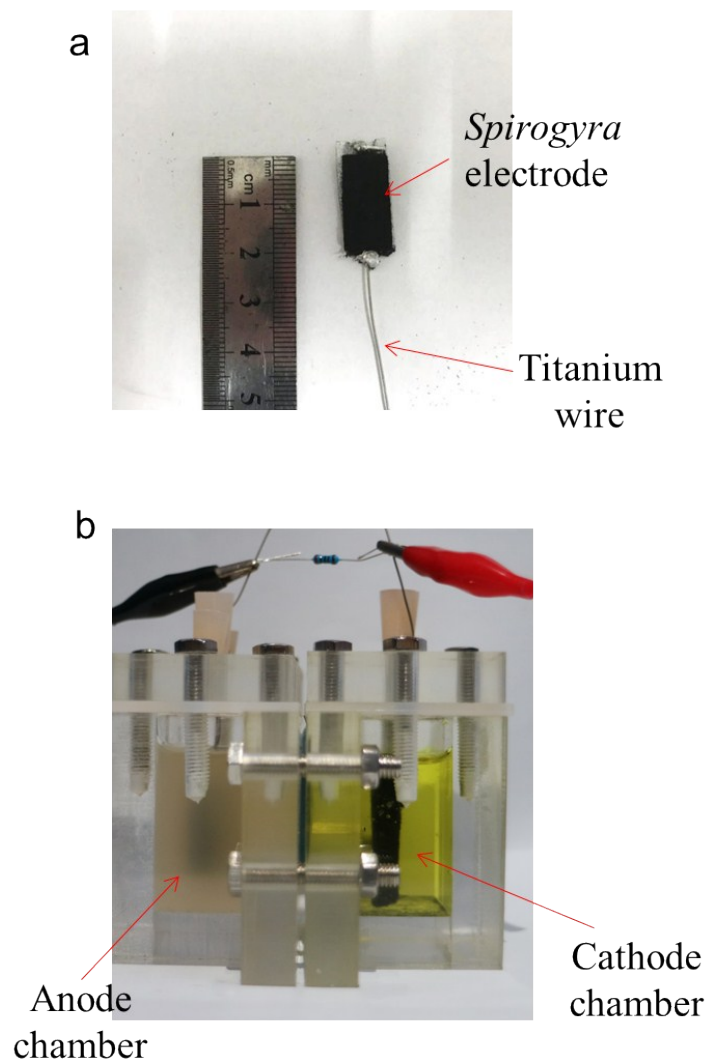


**Figure S10.** (a) Carbonized spirogyra carbon belts derived electrode that wired with titanium wire for MFCs applications. (b) Picture of dual chamber MFC used in this study. Possible electrochemical interference to MFCs performance from the electrodes was excluded: the MFCs with spirogyra electrode but without bacteria inoculation showed no significant voltage and power output.

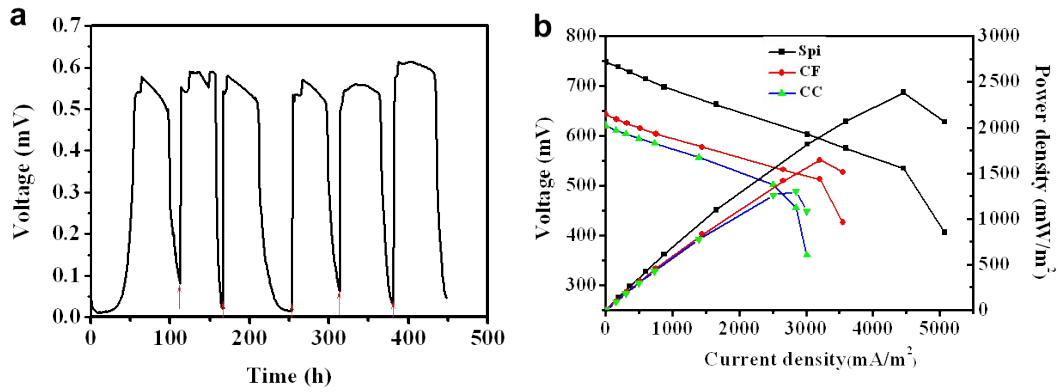


**Figure S11.** (a) Long-term discharge curve of MFC equipped with spirogyra derived electrode by using activated sludge as the inoculum. Red arrows indicate substrate refreshment. (b) Polarization curves and power density curves for MFCs with different electrodes by using activated sludge as the inoculum. The MFCs inoculation with activated sludge was performed according to previous reports (*Environ. Sci. Technol.*, 2013, **47**, 14525-14532; *Nano Energy.*, 2014, **10**, 268-276). The activated sludge was collected from local wastewater treatment plant. The MFCs were operated at 30 °C with 1 k $\Omega$  external resistor.

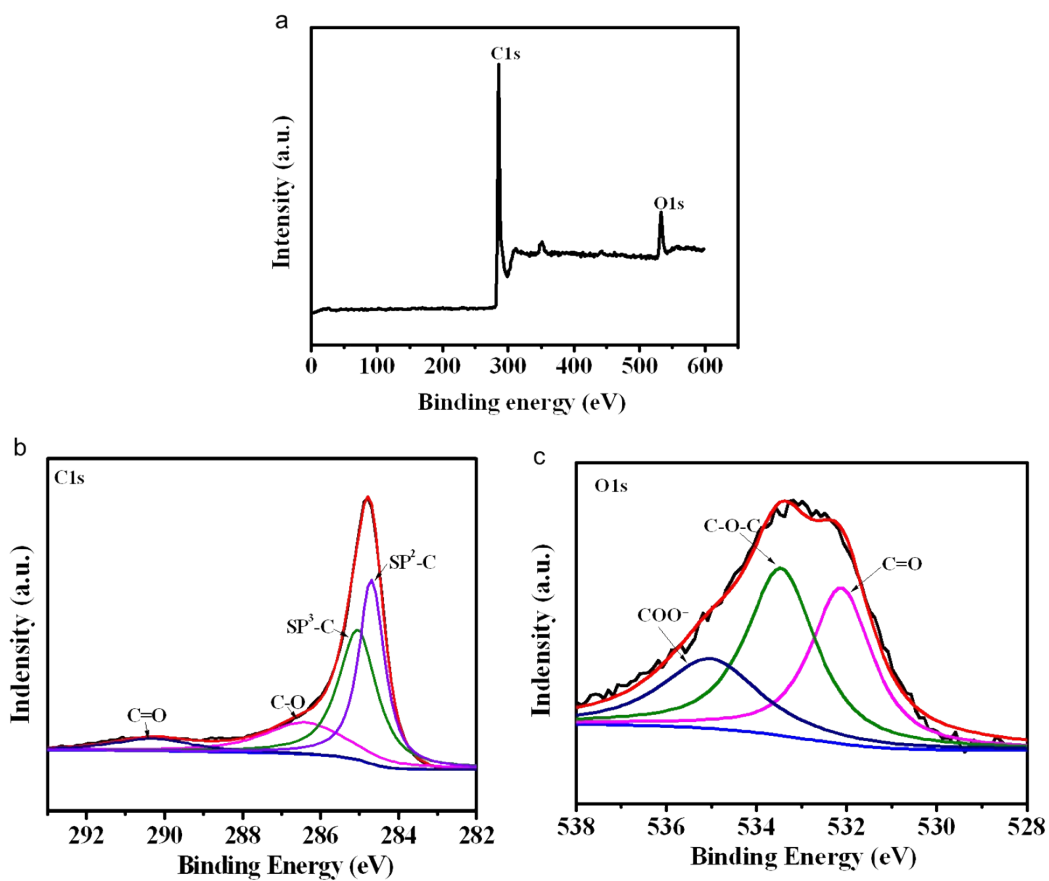


**Figure S12.** (a) Full-scan XPS survey, (b) high resolution spectra of C1s XPS peak and (c) O1s XPS peak of the carbonized spirogyra carbon belts.

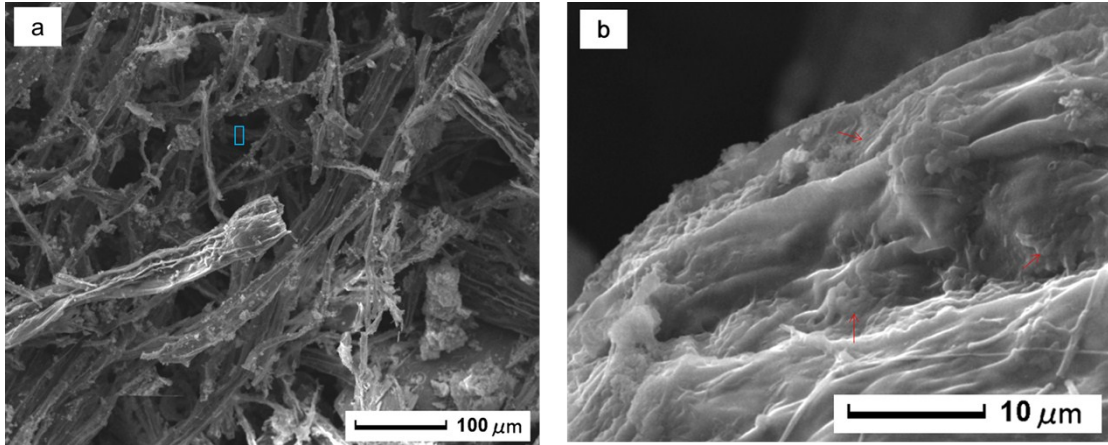


**Figure S13.** SEM images of the biofilm colonized on the spirogyra carbon belts of electrode interior after MFC discharge. In order to observe the biofilm colonized in the electrode interior, the carbon belts of the exterior of spirogyra electrode were removed during SEM sample preparation. Blue frame (a) indicates the area selected for magnification (b). Red arrows indicates the biofilm colonized on the surface of carbon belt that from the electrode interior.

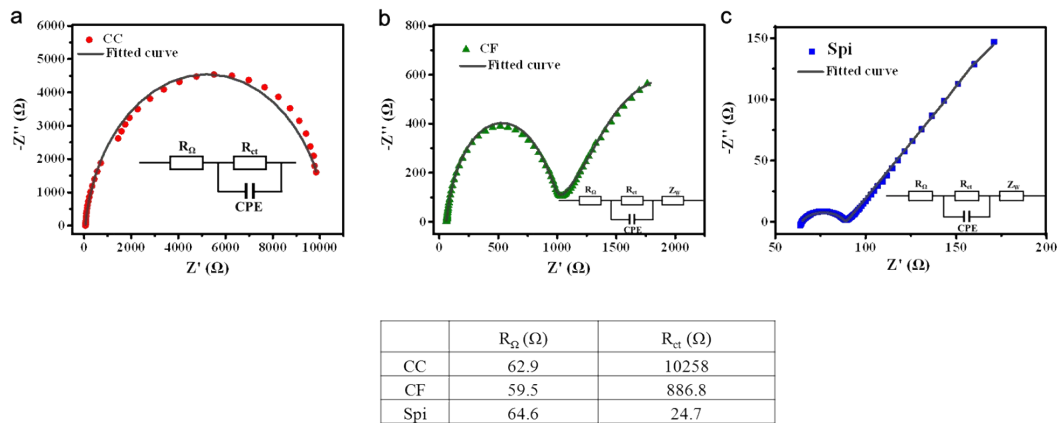


**Figure S14.** Nyquist plots of EIS data fitting with equivalent circuits. Solid dots indicate experimental data, solid lines indicate fitting curves to the equivalent circuits obtained with ZSimpwin program.  $R_{\Omega}$ , ohmic resistance;  $R_{ct}$ , charge transfer/activation resistance; CPE, constant phase element;  $Z_w$ , Warburg element.

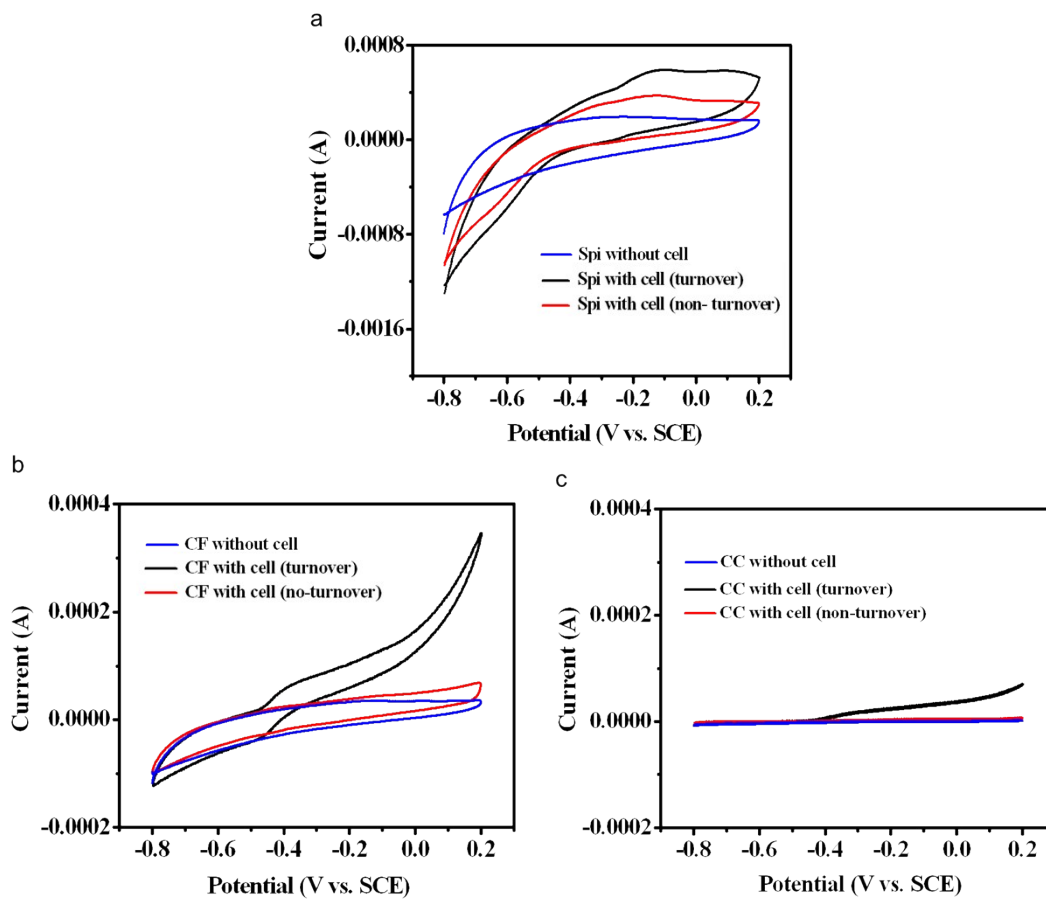


**Figure S15.** CV curves of different electrodes in MFCs. Scan rate is 1 mV/s. Spi: spirogyra derived electrode; CC: carbon cloth electrode; CF: carbon felt electrode.

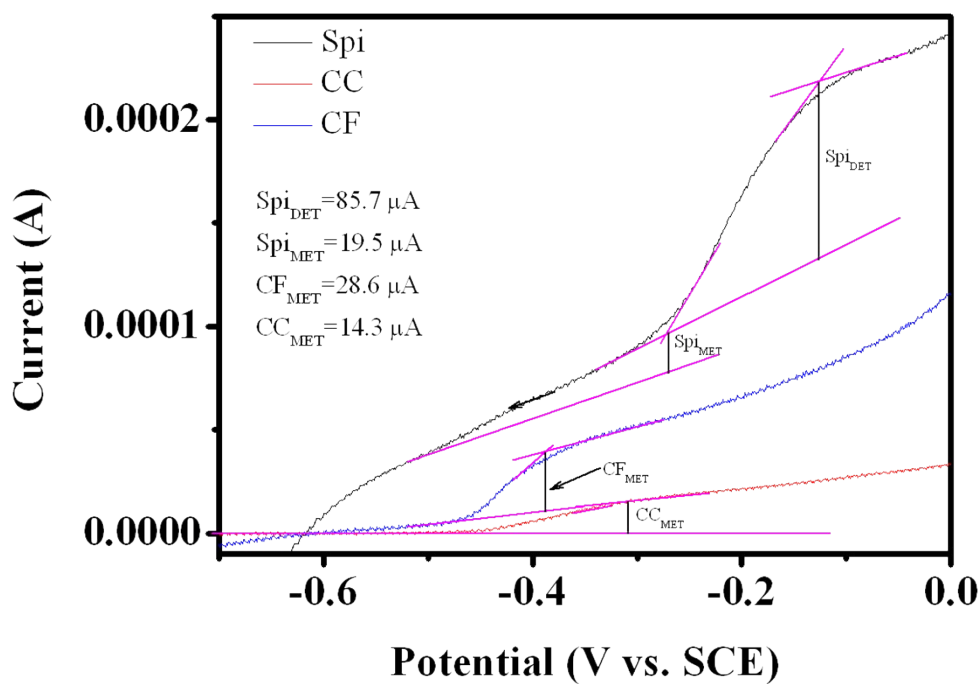


**Figure S16.** The enlarged view of the anodic CV curve of Fig. 5b for catalytic current estimation. Spi: spirogyra derived electrode; CC: carbon cloth electrode; CF: carbon felt electrode. The pink lines were the auxiliary lines added to help catalytic current estimation.